

Spontaneous charge carrier localization in extended one-dimensional systems

Vojtěch Vlček,^{1,2} Helen R. Eisenberg,¹ Gerd Steinle-Neumann,² Daniel Neuhauser,³ Eran Rabani,^{4,5} and Roi Baer¹

¹*Fritz Haber Center for Molecular Dynamics, Institute of Chemistry,
The Hebrew University of Jerusalem, Jerusalem 91904, Israel*

²*Bayerisches Geoinstitut, Universität Bayreuth, 95440 Bayreuth, Germany*

³*Department of Chemistry and Biochemistry, University of California, Los Angeles California 90095, U.S.A.*

⁴*Department of Chemistry, University of California and Materials Science Division,
Lawrence Berkeley National Laboratory, Berkeley, California 94720, U.S.A.*

⁵*The Sackler Center for Computational Molecular and Materials Science, Tel Aviv University, Tel Aviv, Israel 69978*

(Dated: March 24, 2022)

Charge carrier localization in extended atomic systems has been described previously as being driven by disorder, point defects or distortions of the ionic lattice. Here we show for the first time by means of first-principles computations that charge carriers can spontaneously localize due to a purely electronic effect in otherwise perfectly ordered structures. Optimally-tuned range-separated density functional theory and many-body perturbation calculations within the GW approximation reveal that in trans-polyacetylene and polythiophene the hole density localizes on a length scale of several nanometers. This is due to exchange-induced translational symmetry breaking of the charge density. Ionization potentials, optical absorption peaks, excitonic binding energies and the optimally-tuned range parameter itself all become independent of polymer length as it exceeds the critical localization scale. Moreover, lattice disorder and the formation of a polaron result from the charge localization in contrast to the traditional view that lattice distortions precede charge localization. Our results can explain experimental findings that polarons in conjugated polymers form instantaneously after exposure to ultrafast light pulses.

Spatial localization in extended systems has been a central topic in physics, since the pioneering work of Anderson [1] and Mott [2], and more recently in the context of many-body localization [3]. It also forms an important theme in materials science of extended conjugated systems where the dynamics of charges carrier are described in terms of localized polarons. [4–10]. One way to identify charge localization is through the dependence of its energy (e.g., ionization potential or electron affinity) on the system size L . In 1D systems, if the charge remains delocalized, then according to a simple *non-interacting* picture, its energy converges to the bulk limit as $1/L^\alpha$ with $\alpha = 1$ for a metal or $\alpha = 2$ otherwise. However, if the energy becomes independent of L for $L > \ell_c$, it could be due to charge localization within a critical length scale ℓ_c .

Charge localization in conjugated systems can occur in several ways: Attachment by point defects [9], lattice disorder effects [5, 10], and formation of self-bound charged polarons and neutral solitons by local distortion of the nuclear lattice [11–14]. However, it still remains an open question whether localization can occur in disorder-free transitionally invariant systems. This question has received much attention recently in the context of many-body localization [15–18].

In this letter we provide first-principles computational evidence for a new mechanism of localization in 1D conjugated systems, in which the electrons form their own nucleation center without the need to introduce disorder into the Hamiltonian. This challenges the widely accepted picture in which the electronic eigenstates localize only after coupling with the lattice distortion [19]. To

illustrate this mechanism, we study the electronic structure and the charge distribution in large one-dimensional systems with ideal (ordered) geometries. We focus on two representative conjugated polymers, trans-polyacetylene (tPA) and polythiophene (PT), with increasing lengths $L = M\ell_1$ up to $M = 70$ and $M = 20$, respectively (ℓ_1 is the length of the repeat unit). Besides their practical significance [6], they also exhibit interesting physical phenomena, in which polarons, bipolarons and solitons affect charge mobility and localization [4, 12, 20–22].

In Fig. 1 we plot the ionization potentials (IPs) for both the tPA (panel a) and PT (panel b) polymers as a function of the number of repeat units, M . To illustrate the effect of localization we focus on the ionization potential representing the energy of positive charge carrier (hole) rather than on the electron affinity representing the energy of negative charge carrier (electron), since we find the former to localize on shorter length scales (see below). Several levels of theory are used: Hartree-Fock (HF) theory, density functional theory (DFT) within the local density approximation (LDA) [31], the optimally-tuned BNL* [32–34] range-separated hybrid functional [35], and the B3LYP [36] approximation, and, finally, the G_0W_0 many-body perturbation technique [37] (on top of of LDA implemented using stochastic DFT [38]) within the stochastic formulation (*s*GW) [39]. The LDA and to some extent the B3LYP lack sufficient exact exchange while HF lacks correlations and screening effects. BNL* provide a systematic description of correlations and exact exchange through the process of optimal tuning [40]. G_0W_0 is based on many-body perturbation theory and includes exchange, correlation and screening effects [37].

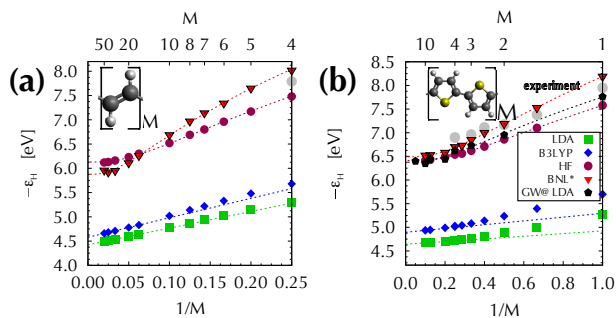


Figure 1. Ionization potentials (estimated using highest occupied eigen-energies ε_H) for (a) trans-polyacetylene and (b) polythiophene shown against the inverse number of repeat units M in the respective polymer. The repeat unit for each polymer is illustrated in the corresponding insets (C, H and S are shown by black, white and yellow spheres, respectively). Results obtained from different computational approaches are indicated by colors and labelled in the figure. Experimental data for the ionization potentials (gray circles) were taken from Refs. 23–25 and references therein. The dashed lines represent a numerical fit to $-\varepsilon_H(M) = -\varepsilon_H(\infty) + \frac{\Delta\varepsilon}{M}$ for LDA and B3LYP ($\varepsilon_H(\infty)$ and $\Delta\varepsilon$ are fitting parameters) and to $-\varepsilon_H(M) = -\varepsilon_H(\infty) + \Delta\varepsilon \exp\left(-\sqrt{M/M_0}\right)$ for HF, BNL*, and GW.

The LDA and B3LYP computations yield IPs that are considerably smaller than the experimental values, consistent with previous computational studies on shorter polymer chains [41, 42] and with general theoretical arguments [43, 44]. These IP values drop to their bulk limit ($I_\infty^{tPA} = 4.4$ eV for tPA and $I_\infty^{PT} = 4.6$ eV for PT) asymptotically linearly as M^{-1} for the range of sizes studied (they do not fit the purely non-interacting asymptotic dependence of M^{-2}). In contrast, HF IPs are significantly closer to the experimental values, deviating by less than 0.4 eV. The HF IPs also initially drop as polymer size increases but for a polymer of length exceeding a critical value, they quickly converge to an asymptotic value, hinting at localization of the hole. The asymptotic HF IPs and HF critical length scale are $I_\infty^{tPA} = 6.1$ eV and $\ell_c^{tPA} = 4.9$ nm and $I_\infty^{PT} = 6.4$ eV and $\ell_c^{PT} = 3.1$ nm (see Supplementary Material for the approach used to determine these quantities). The computational IPs of BNL* and the sGW are in even better agreement with the available experimental data than those of HF. They too show a localization transition with $I_\infty^{tPA} = 5.9$ eV and $\ell_c^{tPA} = 7.9$ nm for tPA and $I_\infty^{PT} = 6.4 - 6.5$ eV and $\ell_c^{PT} = 4.2 - 4.3$ nm for PT. Using the results for intermediate polymers (which do not exhibit localization yet) we can linearly extrapolate to the limit $M \rightarrow \infty$ and estimate the value of ionization potential if no localization occurs; this yields IP values smaller by ≈ 0.5 eV which can be viewed as the energy of spontaneous localization. While the asymptotic values of the ionization potentials predicted by HF, BNL* and sGW are sim-

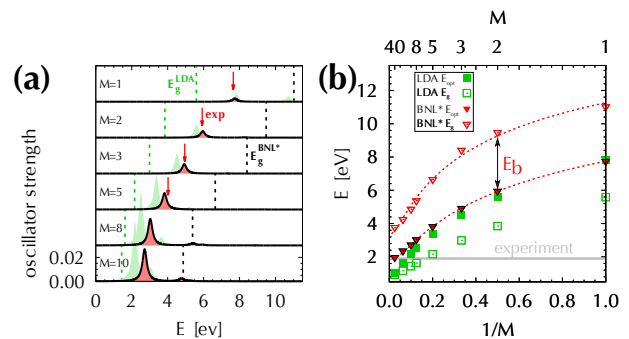


Figure 2. (a) Calculated optical spectra for selected tPA polymers of various lengths (numbers of repeat units M). All calculations were performed with the cc-pvTZ basis set using TDDFT within the BNL* functional (solid black line with red fill) and LDA functional (green filled curve). The fundamental band gaps are shown by dashed vertical lines in corresponding colors. Red arrows indicate experimental absorption peak positions (Refs. 26–29 and references therein). (b) Position of the first maxima of the absorption E_{opt} and the fundamental band gap E_g obtained with BNL* and LDA functionals as function of inverse number of repeat units. Results for the two longest polymers were calculated using the 3-21G basis set, other results are obtained using cc-pvTZ. The exciton binding energy is the difference between E_g and the peak maximum is illustrated by an arrow. The horizontal full line represents the experimental energy of the maximum absorption for the infinite system (1.9 eV) [30].

ilar, the BNL* and sGW critical length scales ℓ_c are larger than those predicted by HF. This result is consistent with the tendency of HF to over-localize holes in finite systems [45, 46].

To further strengthen the validity of the BNL* treatment (and indirectly the G_0W_0 which agrees with the BNL*), we compare its predicted optical excitations E_{opt} and fundamental gaps $E_g = \varepsilon_L - \varepsilon_H$ in tPA to experimental results, where available [26–29] (see Table II of the Supplementary material). The absorption spectra shown in the left panel of Fig. 2 were calculated using time-dependent LDA (ALDA) and BNL* (ABNL*) functionals [33, 47]. It is seen that the ABNL* approach provides excellent agreement for the optical gaps E_{opt}^{ABNL*} in comparison to experimental data. The optical gaps E_{opt} are also plotted as a function of $1/M$ on the right panel of Fig. 2 and it is seen that for the largest system studied the ABNL* optical gap is in excellent agreement with the experimental value [30, 48]. This is in contrast to the ALDA results which underestimate this limit by ≈ 1 eV, and consistently deviate from the ABNL* results as the system size increases. In the right panel of Fig. 2 we also plot the fundamental gap E_g^{BNL*} . The values of E_g^{BNL*} for small systems yields excellent agreement with previous G_0W_0 results [25]. Furthermore, E_g^{BNL*} does not localize for the tPA lengths studied. Since, ε_H^{BNL*} localizes within a length scale of $\ell_c = 7.9$ nm the continued change in E_g^{BNL*} for larger polymers must result from

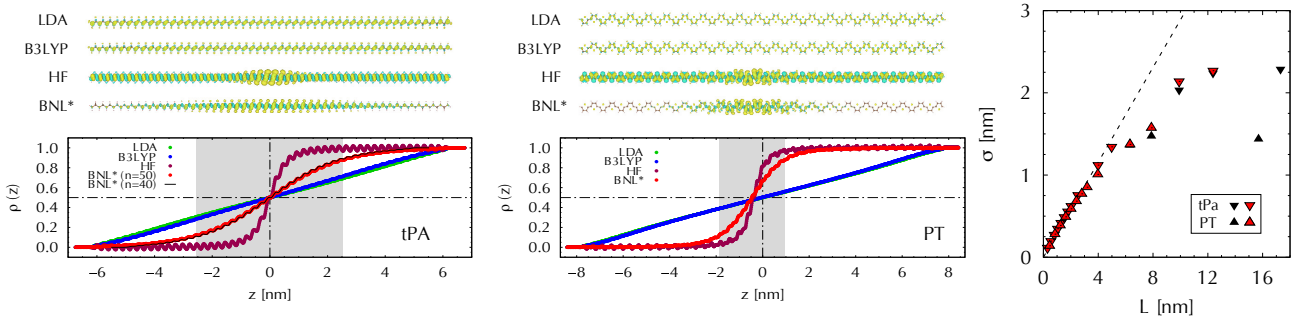


Figure 3. Left panels: The hole densities (top two panels), $\Delta n(\mathbf{r})$, for the corresponding labelled methods in long strands of $M = 50$ repeat tPA units (left) and $M = 20$ repeat PT units (right). The hole is shown as a yellow (aqua) $0.00025a_0^{-3}$ ($-0.00025a_0^{-3}$) density isosurface. In the two bottom left panels we plot the cumulative density, $\rho(z)$, for different functionals. The cumulative curve for a shorter tPA polymer with $M = 40$ (black line) is practically indistinguishable from $M = 50$. Gray areas in the plots show the value of the second cumulant (σ) for the corresponding BNL* hole density, which are plotted in the right panel for different polymer lengths. The dashed straight line in the right panel is the fully delocalized result ($\sigma = L/\sqrt{12}$). Note that for the larger system we used a smaller basis (3-21G, black symbols) which closely follow the results using a larger basis (cc-pvTZ, red symbols).

a continued change in the electron energy $\varepsilon_L^{BNL^*}$. This suggests that negative added charge does not yet localize for the tPA sizes studied and may explain why the finite size gaps are larger than the G_0W_0 gap of 2.1 eV for $L \rightarrow \infty$ [20, 49, 50]. Note, however, that the G_0W_0 gaps are rather sensitive to the size of the unit cell and small changes of 0.005 nm in the position of the atoms can lead to significant fluctuation of 2.0 to 4.2 eV in the gaps [51]. Since there are no experimental measurements of the fundamental gap when $L \rightarrow \infty$, it still remains an open question as to the length scale at which *electrons* localize (as opposed to hole localization, which already occurs at the system sizes studied). To reach system sizes at which the electron localizes will probably require using a stochastic approach for BNL* [52]. Finally, panel a of Fig. 2 shows that the exciton binding energy $E_b = E_g - E_{opt}$ is on the order of $E_g/2$ for the larger systems, a value typical of other 1D conjugated systems [53], indicating that neutral excitations are dominated by electron-hole interactions.

Up to now we have studied localization only from the point of view of energy changes. It is instructive to also study localization in terms of the *hole density*, which is the difference $\Delta n(\mathbf{r}) = n^N(\mathbf{r}) - n^{N-1}(\mathbf{r})$ between the ground state density of the neutral (N) and the ground state density of the positively charged ($N - 1$) systems. For non-interacting electrons this quantity equals the density of the highest occupied eigenstate, which is not localized. However, for interacting electrons $\Delta n(\mathbf{r})$ must be calculated as the difference of densities obtained from two *separate* self-consistent field DFT calculations and can thus exhibit a different behavior. We have also ascertained that the same localization pattern emerges even when an infinitesimal charge $q \rightarrow 0$ is removed, showing that localization of the hole density occurs even also in the linear response regime.

The isosurface plots of the hole densities are given in

the upper left and middle panels of Fig. 3 for the various methods (excluding *s*GW). In the lower left and middle panels we show the *cumulative* hole densities $\rho(z) = \int_{-\infty}^z dz' \int_{-\infty}^{\infty} dy' \int_{-\infty}^{\infty} dx' \Delta n(\mathbf{r}')$. In both types of plots it is evident that LDA and B3LYP do not show localization of the hole density in any of the systems studied and in $\rho(z)$ they show a linear monotonic increase. Contrarily, the HF and BNL* charge distributions localize as observed by change of $\rho(z)$ near the center of the chain. In PT this transition in $\rho(z)$ occurs around one of the S atoms closest to the center of the polymer, due to the lack of mirror plane symmetry. For long polymers exceeding ℓ_c , the BNL* hole density hardly changes as seen by the overlapping $\rho(z)$ of polymers with $M = 40$ and $M = 50$. This implies that the size of the hole is no longer influenced by the polymer terminal points and is thus independent of system size.

The extent of hole localization can be described by the second cumulant $\sigma = \sqrt{\int \Delta n(\mathbf{r}') (z' - \bar{z})^2 d\mathbf{r}'}$ (where $\bar{z} = \int \Delta n(\mathbf{r}') z' d\mathbf{r}'$). This is shown in the right panel of Fig. 3 for BNL*. For small sizes σ increases as $L/\sqrt{12}$, consistent with a uniform hole density spread over the entire polymer. As L increases beyond ℓ_c , the BNL* σ converge to an asymptotic value, σ_∞ , while those of LDA continue to follow the linear $L/\sqrt{12}$ law (not shown).

It is important to note that the hole density $\Delta n(\mathbf{r})$ is dominated by the minority-spin density changes: the orbitals having the same spin as the removed electron redistribute such as to localize the hole density near the chain center. On the other hand, the majority-spin orbitals remain nearly unperturbed and thus do not contribute to $\Delta n(\mathbf{r})$. This fact reveals that the localization is driven by attractive non-local exchange interactions existing solely between like-spin electrons. This is further supported by the fact that localization only appears in methods that

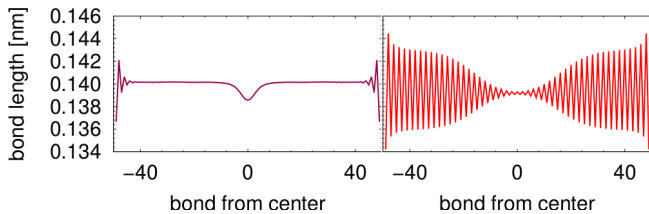


Figure 4. The C-C bond length in the charged $M = 50$ tPA polymer as predicted by HF (left panel) and BNL* (right panel) obtained with the 3-21G basis set. In BNL*, a polaron appears as a reduction of the bond-length alternation, while in the region about 40 C-C bonds away from the polaron, the alternation is increased to 0.007 nm, similar to the experimental value of 0.008 nm for neutral chains [59].

account for non-local exchange (HF, BNL*, and G_0W_0).

One of the interesting ramifications of the IP stabilization as polymer length exceeds a critical length scale is the simultaneous stabilization of the BNL* range-separation parameter γ . This is because in the absence of hole localization the tuning criterion, [40] $I + \varepsilon_H = 0$ is expected to become automatically satisfied when (semi)local functionals are used in the limit of infinite system size [45, 54–56] forcing γ (and with it the non-local exchange part of the functional) to drop eventually to zero. In the systems studied here localization saves the day for tuning and the range parameter attains finite asymptotic values of $\gamma^{tPA} = 2.7 \text{ nm}^{-1}$ and $\gamma^{PT} = 3.1 \text{ nm}^{-1}$. The leveling of γ with L was reported for PT [57], however, it was not previously clear whether γ would level-off for tPA. It is worth pointing out that γ does not change significantly ($< 0.2 \text{ nm}^{-1}$) when LYP correlation is used instead of LDA in the BNL* calculation.

While HF supports partial localization, its hole density also exhibits oscillations along the entire polymer length that do not diminish with system size. These indicate a rigid shift of charge between neighboring atoms: From double to single C-C bonds in tPA and from S to nearby C atoms for PT. This is consistent with the tendency of HF to eliminate bond-length alternation in the entire tPA polymer chain [58] as shown in the left panel of Fig. 4. BNL* on the other hand eliminates the bond-length alternation only in proximity of the localized hole density (right panel of Fig. 4), consistent with a localized polaron model.

In summary, using first principles density functional theory and many-body perturbation theory, we have shown that positive charge carriers can localize in 1D conjugated polymers due to a spontaneous, purely electronic symmetry breaking transition. In this case, localization is driven by non-local exchange interactions and thus cannot occur when (semi)local density functional approximations are used. HF theory, which has non-local exchange, shows a localization transition in a relatively

small length-scale but predicts complete annihilation of bond-length alternation upon ionization, irrespective of polymer length. BNL*, which through tuning includes a balanced account of local and non-local exchange effects, provides an accurate description of the optical gap in comparison to experiments and shows a localization transition with a length scale (estimated from the leveling off of the IPs) that agrees well with the sGW approach. Moreover, BNL* predicts a localized disruption of the bond-length alternation.

The localization phenomenon is driven by the same-spin attractive non-local exchange interactions and therefore, cannot be explained in terms of classical electrostatics. There is no reason to assume that the observed emergence of the localization length ℓ_c in finite systems will not readily occur also in infinite systems, where hole states near the top of the valence band are necessarily infinitely degenerate.

We thank professors Ulrike Salzner and Leor Kronik for illuminating discussions on polymers and localization in large systems. R.B. and E.R. are supported by The Israel Science Foundation–FIRST Program (Grant No. 1700/14). V.V. is supported by Minerva Stiftung of the Max Planck Society, R.B. gratefully acknowledges support for his sabbatical visit by the Pitzer Center and the Kavli Institute of the University of California, Berkeley. D.N. and E.R. acknowledge support by the NSF, grants CHE-1112500 and CHE-1465064, respectively. This research used resources of the National Energy Research Scientific Computing Center, a DOE Office of Science User Facility supported by the Office of Science of the U.S. Department of Energy under Contract No. DE-AC02-05CH11231, and at the Leibniz Supercomputing Center of the Bavarian Academy of Sciences and the Humanities.

-
- [1] P. W. Anderson, *Phys. Rev.* **109**, 1492 (1958).
 - [2] N. F. Mott, *Rev. Mod. Phys.* **40**, 677 (1968).
 - [3] D. Basko, I. Aleiner, and B. Altshuler, *Ann. Phys.* **321**, 1126 (2006).
 - [4] R. H. Friend, R. W. Gymer, A. B. Holmes, J. H. Burroughes, R. N. Marks, C. Taliani, D. D. C. Bradley, D. A. Dos Santos, J. L. Bredas, M. Lögdlund, and Others, *Nature* **397**, 121 (1999).
 - [5] T. Brandes and S. Kettemann, *Anderson Localization and Its Ramifications: Disorder, Phase Coherence, and Electron Correlations*, Vol. 630 (Springer Science & Business Media, 2003).
 - [6] G. D. Scholes and G. Rumbles, *Nat. Mater.* **5**, 683 (2006).
 - [7] J. E. Johns, E. A. Muller, J. M. J. Frechet, and C. B. Harris, *J. Am. Chem. Soc.* **132**, 15720 (2010).
 - [8] D. P. McMahan and A. Troisi, *ChemPhysChem* **11**, 2067 (2010).
 - [9] M. Lannoo, *Point defects in semiconductors I: theoretical aspects*, Vol. 22 (Springer Science & Business Media,

- 2012).
- [10] R. Noriega, J. Rivnay, K. Vandewal, F. P. Koch, N. Stingelin, P. Smith, M. F. Toney, and A. Salleo, *Nature materials* **12**, 1038 (2013).
- [11] W. Kurlancheek, R. Lochan, K. Lawler, and M. Head-Gordon, *J. Chem. Phys.* **136**, 054113 (2012).
- [12] U. Salzner, *Wiley Interdiscip. Rev. Comput. Mol. Sci.* **4**, 601 (2014).
- [13] T. Körzdörfer and J.-L. Brédas, *Acc. Chem. Res.* **47**, 3284 (2014).
- [14] A. Köhler and H. Bässler, *Electronic Processes in Organic Semiconductors: An Introduction* (John Wiley & Sons, 2015) p. 424.
- [15] N. Yao, C. Laumann, J. I. Cirac, M. Lukin, and J. Moore, arXiv preprint arXiv:1410.7407 (2014).
- [16] W. De Roeck and F. Huveneers, *Phys. Rev. B* **90**, 165137 (2014).
- [17] J. M. Hickey, S. Genway, and J. P. Garrahan, arXiv preprint arXiv:1405.5780 (2014).
- [18] M. Schiulaz, A. Silva, and M. Müller, *Phys. Rev. B* **91**, 184202 (2015).
- [19] T. Holstein, *Ann. Phys. (N. Y.)* **8**, 325 (1959).
- [20] P. Puschnig and C. Ambrosch-Draxl, *Synth. Met.* **135-136**, 415 (2003).
- [21] I. H. Nayyar, E. R. Batista, S. Tretiak, A. Saxena, D. L. Smith, and R. L. Martin, *J. Phys. Chem. Lett.* **2**, 566 (2011).
- [22] S. T. Hoffmann, F. Jaiser, A. Hayer, H. Bässler, T. Unger, S. Athanasopoulos, D. Neher, and A. Köhler, *J. Am. Chem. Soc.* **135**, 1772 (2013).
- [23] D. Jones, M. Guerra, L. Favaretto, A. Modelli, M. Fabrizio, and G. Distefano, *J. Phys. Chem.* **94**, 5761 (1990).
- [24] D. A. d. S. Filho, V. Coropceanu, D. Fichou, N. E. Gruhn, T. G. Bill, J. Gierschner, J. Cornil, and J.-L. Brédas, *Philos. Trans. A. Math. Phys. Eng. Sci.* **365**, 1435 (2007).
- [25] M. Pinheiro, M. J. Caldas, P. Rinke, V. Blum, and M. Scheffler, *Phys. Rev. B* **92**, 195134 (2015), arXiv:1503.03704.
- [26] R. McDiarmid, *J. Chem. Phys.* **64**, 514 (1976).
- [27] W. M. Flicker, O. A. Mosher, and A. Kuppermann, *Chem. Phys. Lett.* **45**, 492 (1977).
- [28] K. L. D'Amico, C. Manos, and R. L. Christensen, *J. Am. Chem. Soc.* **102**, 1777 (1980).
- [29] J. L. Bredas, R. Silbey, D. S. Boudreaux, and R. R. Chance, *J. Am. Chem. Soc.* **105**, 6555 (1983).
- [30] A. Feldblum, J. H. Kaufman, S. Etemad, A. J. Heeger, T. C. Chung, and A. G. MacDiarmid, *Phys. Rev. B* **26**, 815 (1982).
- [31] J. P. Perdew and Y. Wang, *Phys. Rev. B* **45**, 13244 (1992).
- [32] R. Baer and D. Neuhauser, *Phys. Rev. Lett.* **94**, 043002 (2005).
- [33] R. Baer, E. Livshits, and U. Salzner, *Annu. Rev. Phys. Chem.* **61**, 85 (2010).
- [34] L. Kronik, T. Stein, S. Refaely-Abramson, and R. Baer, *J. Chem. Theory Comput.* **8**, 1515 (2012).
- [35] A. Savin and H.-J. Flad, *Int. J. Quantum Chem.* **56**, 327 (1995).
- [36] A. D. Becke, *J. Chem. Phys.* **98**, 5648 (1993).
- [37] M. S. Hybertsen and S. G. Louie, *Phys. Rev. B* **34**, 5390 (1986).
- [38] R. Baer, D. Neuhauser, and E. Rabani, *Phys. Rev. Lett.* **111**, 106402 (2013).
- [39] D. Neuhauser, Y. Gao, C. Arntsen, C. Karshenas, E. Rabani, and R. Baer, *Phys. Rev. Lett.* **113**, 076402 (2014).
- [40] E. Livshits and R. Baer, *Phys. Chem. Chem. Phys.* **9**, 2932 (2007).
- [41] U. Salzner, *J. Phys. Chem. A* **114**, 10997 (2010).
- [42] U. Salzner and A. Aydin, *J. Chem. Theory Comput.* **7**, 2568 (2011).
- [43] U. Salzner and R. Baer, *J. Chem. Phys.* **131**, 231101 (2009).
- [44] T. Stein, J. Autschbach, N. Govind, L. Kronik, and R. Baer, *J. Phys. Chem. Lett.* **3**, 3740 (2012).
- [45] P. Mori-Sánchez, A. J. Cohen, and W. Yang, *Phys. Rev. Lett.* **100** (2008), 10.1103/PhysRevLett.100.146401, arXiv:0708.3688.
- [46] E. Livshits and R. Baer, *J. Phys. Chem. A* **112**, 12789 (2008).
- [47] T. Stein, L. Kronik, and R. Baer, *J. Am. Chem. Soc.* **131**, 2818 (2009).
- [48] G. Leising, *Phys. Rev. B* **38**, 10313 (1988).
- [49] M. Rohlfing and S. G. Louie, *Phys. Rev. Lett.* **82**, 1959 (1999).
- [50] S. Rohra, E. Engel, and A. Görling, *Phys. Rev. B* **74**, 045119 (2006).
- [51] A. Ferretti, G. Mallia, L. Martin-Samos, G. Bussi, A. Ruini, B. Montanari, and N. M. Harrison, *Phys. Rev. B* **85**, 235105 (2012).
- [52] D. Neuhauser, E. Rabani, Y. Cytter, and R. Baer, *J. Phys. Chem. A* (2015).
- [53] F. Wang, G. Dukovic, L. E. Brus, and T. F. Heinz, *Science* **308**, 838 (2005).
- [54] R. W. Godby and I. D. White, *Phys. Rev. Lett.* **80**, 3161 (1998).
- [55] S. Ögüt, J. R. Chelikowsky, and S. G. Louie, *Phys. Rev. Lett.* **79**, 1770 (1997).
- [56] V. Vlček, H. R. Eisenberg, G. Steinle-Neumann, L. Kronik, and R. Baer, *J. Chem. Phys.* **142**, 034107 (2015).
- [57] T. Körzdörfer, J. S. Sears, C. Sutton, and J.-L. Brédas, *J. Chem. Phys.* **135**, 204107 (2011).
- [58] L. Rodrigues-Monge and S. Larsson, *J. Chem. Phys.* **102**, 7106 (1995).
- [59] C. S. Yannoni and T. C. Clarke, *Phys. Rev. Lett.* **51**, 1191 (1983).